

(19) World Intellectual Property Organization  
International Bureau



(43) International Publication Date  
22 May 2003 (22.05.2003)

PCT

(10) International Publication Number  
**WO 03/041632 A2**

(51) International Patent Classification<sup>7</sup>: **A61J**

(21) International Application Number: PCT/US02/33640

(22) International Filing Date:  
14 November 2002 (14.11.2002)

(25) Filing Language: English

(26) Publication Language: English

(30) Priority Data:  
60/331,292 14 November 2001 (14.11.2001) US

(71) Applicant: **TEXAS TECH UNIVERSITY** [US/US];  
Texas Tech University Health Sciences Center, P.O. Box  
42007, Lubbock, TX 79409-2007 (US).

(72) Inventors: **KHAN, Mansoor, A.**; Texas Tech School of  
Pharmacy, 1300 Coulter, Amarillo, TX 79106 (US). **NAZ-**  
**ZAL, Sami**; Texas Tech School of Pharmacy, 1300 Coulter,  
Amarillo, TX 79106 (US).

(74) Agent: **YANCY, Jennifer, P.**; Jones, Tullar & Cooper,  
P.C., P.O. Box 2266, Eads Station, Arlington, VA 22202  
(US).

(81) Designated States (*national*): AE, AG, AL, AM, AT, AU,  
AZ, BA, BB, BG, BR, BY, BZ, CA, CH, CN, CO, CR, CU,  
CZ, DE, DK, DM, DZ, EC, EE, ES, FI, GB, GD, GE, GH,  
GM, HR, HU, ID, IL, IN, IS, JP, KE, KG, KP, KR, KZ, LC,  
LK, LR, LS, LT, LU, LV, MA, MD, MG, MK, MN, MW,  
MX, MZ, NO, NZ, OM, PH, PL, PT, RO, RU, SD, SE, SG,  
SI, SK, SL, TJ, TM, TN, TR, TT, TZ, UA, UG, UZ, VC,  
VN, YU, ZA, ZM, ZW.

(84) Designated States (*regional*): ARIPO patent (GH, GM,  
KE, LS, MW, MZ, SD, SL, SZ, TZ, UG, ZM, ZW),  
Eurasian patent (AM, AZ, BY, KG, KZ, MD, RU, TJ, TM),  
European patent (AT, BE, BG, CH, CY, CZ, DE, DK, EE,  
ES, FI, FR, GB, GR, IE, IT, LU, MC, NL, PT, SE, SK,  
TR), OAPI patent (BF, BJ, CF, CG, CI, CM, GA, GN, GQ,  
GW, ML, MR, NE, SN, TD, TG).

**Published:**

— *without international search report and to be republished  
upon receipt of that report*

*For two-letter codes and other abbreviations, refer to the "Guid-  
ance Notes on Codes and Abbreviations" appearing at the begin-  
ning of each regular issue of the PCT Gazette.*



**WO 03/041632 A2**

(54) Title: EUTECTIC-BASED SELF-NANOEMULSIFIED DRUG DELIVERY SYSTEM

(57) Abstract: A eutectic-based self-nanoemulsified drug delivery system (SNEDDS) is formulated from polyoxyl (35) castor oil (Cremophor), medium chain mono- and diglycerides (capmul), essential oils, and a pharmacologically effective drug. The preferred pharmacologically effective drug is a poorly water soluble drug, such as ubiquinone (CoQ<sub>10</sub>). The SNEDDS can be further incorporated into a powder to produce a solid dosage form. The solid dosage form contains the SNEDDS, a copolymer of vinylpyrrolidone and vinyl acetate (Kollidon VA 64), maltodextrin, and microcrystalline cellulose (MCC).

## EUTECTIC-BASED SELF-NANOEMULSIFIED DRUG DELIVERY SYSTEM

## CROSS-REFERENCE TO RELATED APPLICATIONS

- [0001] This application claims the benefit, under 35 U.S.C. 119(e), of U.S. Provisional Application No. 60/331,292 filed November 14, 2001, the contents of which are incorporated herein by reference.

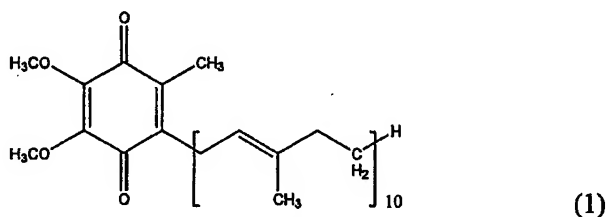
## BACKGROUND OF THE INVENTION

## 1. Field of the Invention

- [0002] The present invention relates generally to a eutectic-based self-nanoemulsified drug delivery system (herein referred to as "SNEDDS"). The eutectic-based SNEDDS is preferably used to administer poorly water soluble drugs to a patient.

## 2. Description of Related Art

- [0003] Large proportions of new drug candidates have poor water solubility. To overcome these problems, various formulation strategies were reported, including complexation with cyclodextrin, solid dispersions and co-precipitates. In recent years, however, much attention has been focused on lipid based formulations, with particular emphasis on self-emulsifying drug delivery systems (herein referred to as "SEDDS"). SEDDS are isotropic mixtures of oil, surfactant, co-surfactant and drug that form fine oil-in-water emulsion when introduced into aqueous medium under gentle agitation.
- [0004] Ubiquinone, also known as Coenzyme Q<sub>10</sub> (herein referred to as "CoQ<sub>10</sub>"), is an important component of the mitochondrial respiratory chain. The structure of CoQ<sub>10</sub> is as follows:



- Because of its poor water solubility, CoQ<sub>10</sub> presents a challenge when developing a formulation for oral administration. Many approaches have been used to improve the in vitro dissolution of CoQ<sub>10</sub>. Some of the approaches include complexation with cyclodextrins, solubilization in a blend of polysorbate 80 and medium chain triglycerides, preparation of redispersible dry emulsion, solid dispersion, and recently, development of a self-emulsified drug delivery system (SEDDS).

[0005] In the traditional methods of preparing self-emulsified delivery systems, active ingredients are dissolved in fixed oils or triglycerides and subsequently blended with suitable solubilizing agents. However, due to limited solubility of some drugs, such as CoQ<sub>10</sub>, in these oils, such methods often result in low drug loading and suffer from irreversible precipitation of the active ingredient and/or the excipient with time.

[0006] Emulsion systems based on a eutectic mixture of lidocaine-prilocaine and lidocaine-menthol were used in preparation of topic formulations. However, little is known about the use of eutectic mixtures for the preparation of self-emulsified formulation.

[0007] Formulations containing SEDDS also require filling into soft or hard gelatin capsules.

10 Therefore, the incorporation of self-emulsifying vehicles into a powder to produce solid dosage forms would be of great interest. Recently, pellets containing a self-emulsifying mixture were prepared by extrusion-spheronization. Solid-state microemulsion for the delivery of cyclosporin also was prepared by coating the premicroemulsion with an enteric material. Similarly, a solvent-evaporation method was used to prepare tocopheryl nicotinate tablets using calcium silicates as the adsorbing agent. Such methods often require elaborate processing and instrumentation.

[0008] On the other hand, solid solutions and liquisols were produced by blending liquid medications with selected powder excipients to produce free-flowing, readily compressible powders. Such excipients include cellulose or lactose as the carriers and fine silicates as the coating material. Using a similar approach, a solid dosage form based on microemulsion adsorbed onto colloidal silicon dioxide and microcrystalline cellulose was introduced. In most cases as well as in the case of liquisols, however, adsorbed oil- or lipid-based formulations form a thin film of oil on the surface of the powder. This film causes particles to adhere and produces a mass that exhibits poor flow and tableting characteristics. To improve flow and compaction properties, oil loading is reduced, or fine particulates such as silicates are added in quantities often exceeding the limits stated by the Code of Federal Regulations.

#### BRIEF SUMMARY OF THE INVENTION

30 [0009] To overcome the foregoing problems, a eutectic-based semisolid self-nanoemulsified drug delivery system (SNEDDS) was formed as an alternative to the conventional self-emulsifying vehicles. The SNEDDS contains polyoxyl 35 castor oil (herein referred to as "Cremophor") as a surfactant, a medium chain mono- and diglyceride (herein referred to as "Capmul") as a co-surfactant, essential oils, and a pharmacologically effective drug. The

preferred amount of Cremophor is 23-31 wt%. The preferred amount of Capmul is 23-31 wt. %. The preferred amount of essential oils is 19-26 wt. %. The preferred amount of the pharmacologically effective drug is 19-26 wt.%. The essential oils are preferably volatile oils selected from the group comprising menthol, spearmint oil, peppermint oil, lemon oil, anise oil and mixtures thereof. Preferably, the pharmacologically effective drug is a drug having poor water solubility. The preferred pharmacologically effective drug is ubiquinone (herein referred to as "CoQ<sub>10</sub>"). The SNEDDS is in the form of a semi-solid mass that is then introduced into soft or hard gelatin capsules.

[0010] A SNEDDS contains an isotropic mixture of oil, surfactant, co-surfactant and drug, which forms a fine oil-in-water emulsion when introduced into an aqueous medium under gentle agitation. In a eutectic-based SNEDDS, the melting point depression method allows the oil phase containing the drug itself to melt at body temperature from its semisolid consistency and disperse to form emulsion droplets in nanometer size range. The SNEDDS improves the dissolution of poorly soluble compounds, such as the preferred CoQ<sub>10</sub>.

[0011] The SNEDDS may be further incorporated into a powder to produce a solid dosage form. The solid dosage form contains the SNEDDS and the following powdered ingredients: a copolymer of vinylpyrrolidone and vinyl acetate (herein referred to as "Kollidon VA 64"), maltodextrin and microcrystalline cellulose (herein referred to as "MCC"). The powder ingredients are added to the SNEDDS to provide a solid dosage form having preferably 3-35 wt.% Kollidon VA 64, 35-82 wt.% maltodextrin, 11-47 wt.% MCC and an effective amount of a SNEDDS for administering said pharmacologically effective drug to a patient.

[0012] In a preferred embodiment, when eutectic-based SNEDDS of CoQ<sub>10</sub> are mixed with small quantities of the Kollidon VA 64 a wax-like copolyvidone paste is formed. Kollidon VA 64 possesses a unique dry-binding capacity. Copolyvidone paste ground with a suitable excipient produces granules with good flow properties that are readily available for direct compression. Maltodextrin was found to be a good grinding agent due to its solubility, particle size, and acceptable adsorbing properties. When compressed, however, the given mixture of the copolyvidone paste and maltodextrin produced soft compacts. Therefore, directly compressible microcrystalline cellulose was added. MCC often is regarded as one of the best excipients for direct compression. Extragranular MCC was shown to increase dissolution rates and compressibility of tablets made by high-shear granulation.

## BRIEF DESCRIPTION OF THE SEVERAL VIEWS OF THE DRAWINGS

[0013] The features and advantages of the present invention will become apparent from the following detailed description of a preferred embodiment thereof, taken in conjunction with the accompanying drawings, in which:

- 5 [0014] FIG. 1 shows DSC thermograms of CoQ<sub>10</sub>, L-menthol, and their binary mixtures (ratios by weight);
- [0015] FIG. 2 is a temperature/composition phase diagram of CoQ<sub>10</sub>-menthol binary system determined by DSC;
- [0016] FIG. 3 shows DSC thermograms of CoQ<sub>10</sub>, peppermint oil, and their binary mixtures
- 10 (ratios by weight);
- [0017] FIG. 4 is a temperature/composition phase diagram of CoQ<sub>10</sub>-essential oil binary systems determined by DSC;
- [0018] FIG. 5 is a pseudo-ternary phase diagram indicating the efficient self-emulsification region;
- 15 [0019] FIG. 6 is a graph showing the effect of surfactant (cremophor EL) to co-surfactant (capmul MCM-C8) ratios on mean droplet size diameter and on NTU<sub>observed</sub> and NTU<sub>plateau</sub> turbidity values;
- [0020] FIG. 7 shows the FT-IR spectra of CoQ<sub>10</sub> and lemon oil, and the effect of re-crystallization on the IR spectra of different CoQ<sub>10</sub> mixtures;
- 20 [0021] FIG. 8 shows turbidity-time profiles: a) turbidity-time profile of three CoQ<sub>10</sub> SNEDDS preparation and b) normalized turbidity-time profiles showing the cumulative percent of CoQ<sub>10</sub> released with time for the three CoQ<sub>10</sub> SNEDDS preparations;
- [0022] FIG. 9 is a graph showing the effect of surfactant (cremophor EL) to co-surfactant (capmul MCM-C8) ratios on lag time to self-emulsification;
- 25 [0023] FIG. 10 is a graph showing the effect of surfactant (cremophor EL) to co-surfactant (capmul MCM-C8) ratios on the emulsification rate;
- [0024] FIG. 11 is a representative load-displacement curve obtained from a three-point flexure test of self-nanoemulsified tablet dosage form;
- [0025] FIG. 12 is a representative surface topography, P, W, and R profiles of self-
- 30 nanoemulsified tablets, obtained by a Mahr perthometer concept surface-measuring instrument;
- [0026] FIG. 13 is an out-of-die Heckel plot of six formulations showing the influence of the added Avicel MCC;

[0027] FIG. 14 is a plot of tablet porosity against compaction pressure showing the compressibility of six self-nanoemulsified powdered formulations with various grades of Avicel MCC;

5 [0028] FIG. 15 is a plot of the natural logarithm of tensile strength against porosity showing the compactibility of six self-nanoemulsified powdered formulations with various grades of Avicel MCC;

[0029] FIG. 16 is a plot of tensile strength against compaction pressure showing the tabletability of six self-nanoemulsified powdered formulation with various grades of Avicel MCC;

10 [0030] FIG. 17 is a plot of the percent friability against compaction pressure of six self-nanoemulsified powdered formulations with various grades of Avicel MCC; and

[0031] FIG. 18 is a dissolution plot showing the cumulative percent of CoQ<sub>10</sub> release with time from six self-nanoemulsified tablet formulations with various grades of Avicel MCC.

15 DETAILED DESCRIPTION OF THE INVENTION

[0032] The present invention is directed to a eutectic-based self-nanoemulsified drug delivery system (herein referred to as "SNEDDS") containing an isotropic mixture of oil, surfactant, co-surfactant and a pharmacologically effective drug. The oil present in the SNEDDS is an essential oil that is a volatile oil, preferably selected from the group comprising menthol, spearmint oil, peppermint oil, lemon oil, anise oil and mixtures thereof. The essential oils in the SNEDDS are present in a preferred amount of 19-26 wt. %. The pharmacologically effective drug present in the SNEDDS is preferably a poorly water soluble compound, preferably selected from the group comprising drugs or dietary supplements, or nutraceuticals with a log p value over 3. Most preferably, the pharmacologically effective drug is ubiquinone (herein referred to as "CoQ<sub>10</sub>"). Other preferred pharmacologically effective drugs include, but are not limited to, cyclosporines and Vitamin E. The preferred amount of the pharmacologically effective drug in the SNEDDS is 19-26 wt.%. The surfactant in the SNEDDS is preferably polyoxyl 35 castor oil (herein referred to as "Cremophor") in a preferred amount of 23-31 wt.%. The co-surfactant in the SNEDDS is preferably a medium chain mono- and diglyceride (hereafter, "Capmul") in a preferred amount of 23-31 wt.%. The preferred ratio of Cremophor to Capmul is 0.5-1.5. A preferred SNEDDS containing 23 wt.% lemon oil, 23 wt.% CoQ<sub>10</sub>, 27 wt.% Cremophor, and 27 wt.% Capmul releases 93.4% CoQ<sub>10</sub>. The SNEDDS produces a semi-solid mass which is filled into soft or hard gelatin

capsules. In a preferred embodiment, the SNEDDS are filled into hydroxypropyl methylcellulose (HPMC) capsules.

[0033] The SNEDDS may be further incorporated into a powder to produce a solid dosage form by combining the SNEDDS with the following powder ingredients: a copolymer of vinylpyrrolidone and vinyl acetate (herein referred to as "Kollidon VA 64"), maltodextrin and microcrystalline cellulose (herein referred to as "MCC"). The preferred MCC is Avicel MCC, which is available in many grades that differ from each other by their particle size, particle shape, and moisture content, obtained from FMC Corp. (Newark, DE). Table 1 shows the physicochemical properties of the preferred Avicel MCC. Avicel PH 105 produces a sustained release tablet dosage form.

Table 1

Avicel MCC Grade	Average Particle Size ( $\mu\text{m}$ )	Moisture Content (%)
Avicel PH-105	20	$\leq 5$
Avicel PH-101	50	$\leq 5$
Avicel PH-113	50	$\leq 2$
Avicel PH-102	90	$\leq 5$
Avicel PH-112	90	$\leq 1.5$
Avicel PH-200	180	$\leq 5$

Various MCC grades with different particle size and moisture contents vary in their adsorbing capacity, as shown below in the preferred embodiment illustrated in Example II. Although an MCC with a smaller particle size such as Avicel PH-105 provides a greater surface area for oil adsorption, it shows a reduction in compatibility and tensile strength. On the other hand, Avicel PH-112, which has larger particles and reduced adsorbing capacity, demonstrated improved hardness and compaction. The initial size of the particles constituting a powder is an important factor in determining its compaction behavior. For most powdered materials, compaction of the small particles results in stronger tablets because of the large surface area available for bonding. The powder ingredients are added to the SNEDDS to provide a solid dosage form having preferably 3-35 wt.% Kollidon VA 64, 35-82 wt.% maltodextrin, 11-47 wt.% MCC, and an effective amount of a SNEDDS for administering said pharmacologically effective drug to a patient. In a preferred embodiment, the optimum amount of SNEDDS added to a solid dosage form is determined by maximizing

the amount of the pharmacologically effective drug emulsified into a dissolution medium within 45 minutes. In a preferred embodiment wherein CoQ<sub>10</sub> is the pharmacologically effective drug, 46.1-91.1 wt.% CoQ<sub>10</sub> was released from the solid dosage form within 45 minutes. A preferred solid dosage form containing 7.8 wt.% Kollidon VA 64, 65.4 wt.% maltodextrin, 11.7 wt.% MCC, and 15.1 wt.% SNEDDS release 85.4% of CoQ<sub>10</sub>. The SNEDDS is this preferred solid dosage form contained an oily mix of CoQ<sub>10</sub> and lemon oil in a ratio of 1:1. Cremophor EL and Capmul MCM-C8 were added to the oily mix at a final concentration of 26.9% w/w each.

10

### EXAMPLE I

[0034] The present example illustrated the use of eutectic mixtures with essential oils for the preparation of SNEDDS. Prepared SNEDDS improve the dissolution of poorly water soluble drugs, such as CoQ<sub>10</sub>. Recrystallization adds to the stability of the drug while providing attractive semisolid preparation that could be filled into hard capsules. Turbidimetry directly correlates emulsification rate, lag times and droplet size with formulation ingredients. This was used to distinguish between different self-emulsified preparations, which might be more important than simply identifying systems that are spontaneously emulsifying.

*Differential scanning calorimetry (DSC) of CoQ<sub>10</sub>- menthol and CoQ<sub>10</sub>-essential oil binary system.*

[0035] CoQ<sub>10</sub> and L-menthol were mixed at various ratios between 90:10 and 10:90 (w/w). Approximately 5 mg of the mixture was sealed in an aluminum pan and analyzed using a differential scanning calorimeter (DSC 7, Perkin-Elmer, Norwalk, CT). Thermal analysis was carried out between 25 and 60 °C under nitrogen gas flow against an empty reference pan at a heating rate of 10 °C min<sup>-1</sup>. Similarly, different ratios of CoQ<sub>10</sub> and the essential oil between 80:20 and 20:80 (w/w) were mixed and melted at 37 °C. Resulting oils were stored at 4 °C for 24 hours to allow complete re-crystallization of CoQ<sub>10</sub>. To avoid oil evaporation, approximately 10 mg of the mixture was weight onto a DSC sample pan and kept in an airtight container during storage prior to DSC analysis. For CoQ<sub>10</sub>-essential oil mixtures at ratios between 80:20 and 60:40 (w/w), thermal analysis was carried out between 25 and 55 °C. Heating rate used was 10 °C min<sup>-1</sup>. Lower temperatures were maintained using refrigerated cooling accessory (Intracooler 2, Perkin-Elmer).

[0036] CoQ<sub>10</sub> was found to form a eutectic mixture with L-menthol. DSC thermograms of the binary system of CoQ<sub>10</sub> with menthol at different ratios are given in FIG. 1. The major endotherms at 51.7 and 44.1 °C represent the melting point of CoQ<sub>10</sub> and L-menthol,



respectively. Based on the thermal analysis data a binary phase diagram was constructed and is given in FIG. 2. As seen from FIG. 2, the eutectic melting point lies between 30 and 60% w/w CoQ<sub>10</sub>. Within the binary system, depression in melting temperature of CoQ<sub>10</sub>, however, was limited to temperatures exceeding 37 °C. Thus, an oily melt can not be obtained at or below body temperature. A gradual shift and reformation of the original CoQ<sub>10</sub> endothermic peak was observed when the samples within the binary system were left uncovered and analyzed after 1 week. The volatile ingredients of menthol are responsible for the physical changes in CoQ<sub>10</sub>, i.e. depression in its melting temperature. To validate this observation, the effect of peppermint oil as a representative volatile ingredient of menthol crystals and three additional volatile oils namely, spearmint oil, lemon oil and anise oil were investigated for their effect on the melting thermograms of CoQ<sub>10</sub>. Thermal analysis and the DSC data of the binary system of CoQ<sub>10</sub> with peppermint oil are given in FIG. 3. A binary phase diagram of CoQ<sub>10</sub> with the essential oils was constructed and is given in FIG. 4. Thermograms of the mixtures clearly indicated that these compounds formed binary eutectic systems. An increase in percent essential oil causes a gradual decrease in the melting temperature of CoQ<sub>10</sub>. At sufficient concentration of the volatile oil it becomes feasible to convert CoQ<sub>10</sub> into an oily phase at or below body temperatures.

#### *Determination of CoQ<sub>10</sub> melting time*

[0037] CoQ<sub>10</sub> was accurately weighed and mixed with 50 and 60% w/w of peppermint oil, spearmint oil, anise oil or lemon oil in a screw-capped glass vials. Mixtures were allowed to melt at 37 °C in water bath (Ikamag® Ret-G, Terochem Scientific, Toronto, Canada). Cremophor EL was added to the melt at a concentration of 20, 40 and 60% w/w of the final weight using a positive displacement pipette (Microman®, Gilson Inc., Middleton, WI) and stirred with a magnetic bar. Vials were then capped and stored at ambient temperatures in tight containers protected from light. After 24 hours sample vials containing the solidified preparation were immersed in water bath maintained at 37 °C. Samples were monitored for a change in their physical appearance and the time was recorded until a complete melt was obtained.

[0038] Due to the limited solubility of CoQ<sub>10</sub> in fixed oils and triglycerides, the melting point depression method using essential oils provides an attractive alternative for the preparation of an emulsified formulation. A number of essential oils are used for their flavors and odors and are recognized by the Code of Federal Regulations as GRAS (generally recognized as safe) compositions that do not require regulatory agency approval before they are included in ingested material. A preparation could be made at which body temperature is used to melt a

system comprising essential oil, CoQ<sub>10</sub> and an emulsifier when the essential oil is added in an amount sufficient to lower the melting temperature of CoQ<sub>10</sub> to or below 37 °C. Essential oils, however, should be effective as eutectic agents in the presence of other liquid excipients. Table 2 demonstrates the feasibility of the described approach by showing the melting time, in minutes, for the given mixture of CoQ<sub>10</sub>, essential oil and cremophor EL at 37 °C. Four essential oils, spearmint oil, peppermint oil, lemon oil, and anise oil, were evaluated for their eutectic efficacy in the presence of other formulation excipients. The essential oil percentage rates in Table 2 are the percent w/w of essential oil in the binary mixture of the essential oil with CoQ<sub>10</sub>. The Cremophor EL (CrEL) percentage rates in Table 2 are the percent w/w of Cremophor EL in the final mixture of CoQ<sub>10</sub>, essential oil and cremophor EL. The N/A indication in Table 1 indicates the formulations where no melting time was observed within 24 hours.

Table 2

CrEL (%)	20%	40%	60%
<i>Spearmint Oil</i>			
60%	0.69 ± 0.13	1.56 ± 0.59	N/A
50%	4.38 ± 2.13	N/A	N/A
<i>Peppermint Oil</i>			
60%	1.11 ± 0.42	N/A	N/A
50%	8.17 ± 2.08	N/A	N/A
<i>Anise Oil</i>			
60%	0.83 ± 0.73	0.97 ± 0.27	N/A
50%	1.28 ± 0.63	2.33 ± 0.88	N/A
<i>Lemon Oil</i>			
60%	1 ± 0.17	1.29 ± 0.44	1.76 ± 0.23
50%	2 ± 0.29	3.56 ± 1.69	5.33 ± 1.48

Due to limited solubility of CoQ<sub>10</sub> in surfactant, the use of cremophor EL as a model emulsifier not only induces crystallization of CoQ<sub>10</sub> in the cooled supersaturated mixture but also may delay or retard re-melting the system at higher temperatures. The time necessary to melt different combinations of CoQ<sub>10</sub>, essential oil and cremophor EL at 37 °C was recorded. When 60% w/w of cremophor EL was added, preparations made with 50 and 60% w/w lemon oil to CoQ<sub>10</sub> melted within 5.3 and 1.8 min, respectively. Precipitation of CoQ<sub>10</sub> at

higher cremophor EL concentration for the formulas made with anise oil, peppermint oil and spearmint oils was however irreversible rendering them less effective for the preparation of emulsified systems. The use of lemon oil appears reasonable and attractive. At 50% w/w of lemon oil to CoQ<sub>10</sub>, formulas would melt within 5 min from initial exposure to body  
5 temperatures. In this case, recrystallization of CoQ<sub>10</sub> becomes advantageous in the production of a stable semisolid product compared with the existing liquid formulas with the potential of irreversible precipitation and separation of the active ingredient due to supersaturation or fluctuation in storage temperatures. Furthermore, lemon oil has been used internally as herbal medicine for acidic disorders such as arthritis and rheumatism with great  
10 benefit in liver congestion.

*Visual observations*

[0039] To assess the self-emulsification properties, formulation (50 mg) pre-melted at 37 °C was introduced into 100 ml of water in a glass Erlenmeyer flask at 25 °C and the contents were gently stirred manually. The tendency to spontaneously form a transparent emulsion  
15 was judged as 'good', and it was judged 'bad' when there was poor or no emulsion formation. Phase diagrams were constructed identifying the good self-emulsifying region. All studies were repeated in triplicates with similar observation being made between repeats.  
[0040] For the development of a self-emulsified formulation, a right blend of low and high HLB surfactants is necessary for the formation of a stable microemulsion. Therefore, a high  
20 HLB surfactant, cremphor EL, and a low HLB co-surfactant, capmul MCM-C8, were selected. A ratio of 50:50 of lemon oil to CoQ<sub>10</sub> was selected as the oil phase. The pseudo ternary phase diagram of the system comprising the surfactant, co-surfactant and the oily phase was constructed and is give in FIG. 5. The area enclosed within the solid line represents the region of self-emulsification. Within this area a ternary mixture forms a fine  
25 oil in water emulsion with only gentle agitation. This is possible as surfactant strongly localized to the surface of the emulsion droplet reduces interfacial free energy and provide a mechanical barrier to coalescence resulting in a thermodynamically spontaneous dispersion. Furthermore, co-surfactants increase interfacial fluidity by penetrating into the surfactant film creating void space among surfactant molecules. Constraints on the formulas were placed so  
30 that the oil phase was not less than 37.5% to ensure melting of the crystallized product based on the early predictions give in Table 2, and did not exceed 63% to ensure efficient CoQ<sub>10</sub> emulsification.

*Emulsion droplet size analysis and turbidity measurements*

[0041] Formulation (50 mg) melted at 37 °C was diluted with water, pre-equilibrated at 37 °C, to 100 ml in an Erlenmeyer flask and gently mixed with hand. The resultant emulsions were evaluated for its droplet size and turbidity as follow.

5 [0042] The droplet size distribution of the resultant emulsions was determined by laser diffraction analysis using Coulter particle size analyzer (Model LS230, Miami, FL), which has a particle size measurement range of 0.04-2000  $\mu\text{m}$ . The sizing of the emulsions was determined in a small volume module. Samples were directly placed onto the module and the data was collected for 60 seconds. Particle size was calculated from the volume size  
10 distribution. All studies were repeated, with good agreement being found between measurements.

[0043] Turbidity of the resultant emulsions given in nephelometric turbidity units (NTU) was measured using HACH turbidimeter (Model 2100-AN, Loveland, CO). Turbidity measurements were performed on 30 ml of the emulsion stored in a clear screw-capped  
15 sample vials. The HACH 2100AN turbidimeter used was carefully calibrated with formalin standards. Accuracy at the lower range of turbidity is essential especially for small and diluted emulsions with high surfactant concentrations. The largest source of error at low turbidities is the stray light, that is, the light that reaches the detector due to sources other than sample turbidity. Accuracy of the HACH 2100AN turbidimeter, as specified by the  
20 manufacturer and based on instrument calibration, is approximately  $\pm 0.01$  NTU with stray light less than or equal to 0.01 NTU.

[0044] The effect of surfactant to co-surfactant ratio on droplet size is given in FIG. 6. At ratios greater than 0.5, globule size was relatively constant at about 100 nm and independent on any component of the ternary system. It was only at ratios smaller than 0.5 when globule  
25 size increased and became greatly dependent on cremophor EL and capmul MCM-C8 concentrations yet independent on the added oil phase. It was reported that the addition of surfactant to the microemulsion systems causes the interfacial film to stabilize and condense, while the addition of co-surfactant causes the film to expand. Comparison of droplet size data with the visual observations shows that good emulsification properties are reflected by the  
30 low globule size with the exception of the formula made with high capmul MCM-C8 to cremophor EL ratios. This reflects the fact that the visual test is a measure of the spontaneity of emulsification rather than a measure of the quality of the formed emulsion.

[0045] Turbidity, given in NTU, was measured for the same samples utilized for particle size analysis. The effect of surfactant to co-surfactant ratio of the emulsified formulas on

NTU<sub>observed</sub> and NTU<sub>plateau</sub> turbidity readings is given in FIG. 6. As seen in the plot, turbidity follows the same trend as droplet size. It has been reported that a linear correlation exists between the intensity of the scattered light and the squared volume of the dispersed droplets. Hence, NTU could be directly used to predict relative droplet size of the emulsion. To give a sense about the clarity of the formulas, turbidity of drinking water ranges from 0 to 1 NTU.

*Fourier transform-infrared spectroscopy (FT-IR)*

[0046] FT-IR spectroscopy was performed using FTIR model Nicolet Impact 410 (Thermo Nicolet, Madison, WI) attached to an attenuated total reflectance (ATR) accessory (DuraSampIR, SensIR Technologies, Danbury, CT). ATR was fitted with a single bounce diamond at 45° internally reflected incident light providing a sampling area of 1 mm in diameter with a sampling depth of several microns. Samples analyzed were CoQ<sub>10</sub> powder, a 50:50 CoQ<sub>10</sub>-lemon oil melt, a solidified 50:50 CoQ<sub>10</sub>-lemon oil mix and a solidified mixture of lemon oil, CoQ<sub>10</sub>, cremophor EL and capmul MCM-C8 at a ratio of 0.5:0.5:1:1. Samples were prepared as described above. A small amount of the sample was directly placed on the diamond disk and scanned for absorbance over the range from 4000 to 500 wavenumbers (cm<sup>-1</sup>) at a resolution of 1 cm<sup>-1</sup>.

[0047] The ease of handling aqueous solutions and semisolid preparations is one of the major advantages of ATR used in conjugation with FT-IR spectrometry. CoQ<sub>10</sub> compatibility with the excipients of self-nanoemulsified preparation can be tested with FT-IR. Absorbance spectrums of CoQ<sub>10</sub> and lemon oil are given in FIG. 7. CoQ<sub>10</sub> spectrum showed several sharp characteristic peaks. The spectrum of the 50:50 melt of CoQ<sub>10</sub> and lemon oil, given in FIG. 7, had features of each of the components with the expected peak broadening due to its amorphous character whereas a sample of the solidified mixture had sharp lines and resembled the CoQ<sub>10</sub> spectrum in every detail. Lemon oil did not change the infrared spectrum of CoQ<sub>10</sub> indicating no chemical interaction in the binary system and that the molecular structure of CoQ<sub>10</sub> remained completely intact. Similarly, when cremophor EL and capmul MCM-C8 were added to the CoQ<sub>10</sub>-lemon oil mix and the solidified mixture was analyzed, the resulting spectrum given in FIG. 7 had the characteristic CoQ<sub>10</sub> bands at 1608 and 1643 cm<sup>-1</sup> corresponding to the benzoquinone ring and the mono substituted isoprenoid units, respectively. The results obtained indicate that CoQ<sub>10</sub> reforms to its original crystalline state when the formulation is allowed to solidify.

*Dissolution and emulsification studies*

[0048] Dissolution profiles of the capsules filled with the self-nanoemulsified formulations were mined using USP XXIII rotating paddle apparatus (VanKel, mod. VK 7000, Cary, NC)

at 37 °C and a rotating speed of 50 rpm in a 900 ml of water. Capsules were held to the bottom of the vessel using copper sinkers. Samples (3 ml) withdrawn after 15 min were filtered using a 10  $\mu$ m VanKel filter and assayed for CoQ<sub>10</sub> by the HPLC method reported in the HPLC analysis section. The dissolution experiments were carried out in triplicates.

- 5 [0049] Turbidity profiles of the capsules filled with the self-emulsified formulations were determined using HACH turbidimeter (Model 2100AN). Low-pressure flow cell was used to allow directly reading samples turbidity associated with capsules subjected to the same dissolution conditions as described above. Two 1/8 in. tygon tubing were connected to the pump attached to the dissolution autosampler (VanKel, mod. VK8000). First tubing was  
10 installed between the pump and the inlet of the flow cell while the other connected the pump to the dissolution vessel. Inlet of the tube connecting pump to the dissolution vessel was covered with a 40  $\mu$ m nylon screen and immersed into the medium so that the sample can be continuously withdrawn from a zone midway between the surface of the medium and the top of the rotating blade. Another tubing was installed to the outlet of the flow cell leading back  
15 to the dissolution vessel. Before starting, deionized water was pumped through the flow cell until a reading below 0.150 NTU was maintained. Throughout the study, dissolution medium was continuously pumped into the flow cell and back to the dissolution vessel. The turbidimeter was set so that a reading was recorded on the attached printer every 15 seconds. Turbidimetry experiments were carried out in triplicates.
- 20 [0050] To assess spontaneity and efficacy of emulsification, turbidity of the dispersion and the relative intensity of the scattered light was correlated with time during the emulsification process. Current design confines to the standard compendia requirements for conducting dissolution experiments. Utilizing the flow through attachment, turbidity was directly measured using standard dissolution apparatus at 37 °C and controlled paddle rotating speed.
- 25 Prepared formulations were filled into hydroxypropyl methylcellulose (HPMC) capsules. HPMC capsules are shown to dissolve at longer times compared with standard gelatin capsules. Average dissolution time for an HPMC capsule size 4, 3 and 0 in water at 37 °C was 300, 250 and 120 s, respectively. Extra time provided by HPMC capsules allows the formula to completely melt at body temperature before its exposure to body fluids.
- 30 Representative dissolution curves monitored by turbidimetry for three formulations are shown in FIG. 8(a). Formulation 19 has 21.4% w/w CoQ<sub>10</sub>, 21.4 % w/w lemon oil, 14.3% w/w Capmul, and 42.9% w/w Cremophor. Formulation 32 has 27.3% w/w CoQ<sub>10</sub>, 27.3% w/w lemon oil, 31.8% w/w Capmul, and 13.6% w/w Cremophor. Formulations 36 has 30.0%

w/w CoQ<sub>10</sub>, 30.0% w/w lemon oil, 30.0% w/w capmul, and 10.0% w/w cremophor. Due to large number of readings obtained, plots of turbidity against emulsification time have the characteristic lag phase, pseudo linear phase and a gradual tailing toward a plateau as the emulsion systems approached equilibrium. Actual cumulative amount of CoQ<sub>10</sub> released after 15 min for the preparations was measured by HPLC. CoQ<sub>10</sub> was completely released and dispersed from all formulations into the medium within 15 minutes.

[0051] CoQ<sub>10</sub> was analyzed at ambient temperature utilizing a C18, 3.9 X 150 mm reverse phase chromatography column (Nova-Pak; Waters, Milford, MA). The mobile phase consisted of methanol:*n*-hexane (9:1) and was pumped at a flow rate of 1.5 ml min<sup>-1</sup>. The Waters HPLC instrument consisted of a 510 pump, 712 WISP autosampler, and a 490E UV detector set at a wavelength of 275 nm. The chromatographic data was managed using STAR 5.3 software (Varian, Walnut Creek, CA).

[0052] NTU values obtained for the solidified samples placed in the dissolution medium at 37 °C after reaching an equilibrium could be termed NTU<sub>plateau</sub>. In order to demonstrate the efficacy of emulsion formation before and after solidification NTU<sub>observed</sub>, which were previously determined for the melted samples while measuring droplet size, could be roughly correlated with NTU<sub>plateau</sub>.

[0053] Lag phase of the turbidity-time profile reflects the time elapsed before the formula is released from the capsule into the dissolution medium. FIG. 9 correlates lag times with surfactant to co-surfactant ratios. Intercept of the regression line with the y-axis was at 4.98 min which is almost identical to the average break time for an empty HPMC capsule size 4. Any deviation from this time should be correlated with the inherent properties of the fill material. Increase in cremophor EL to capmul MCM ratios from 0.5 to 3 delayed the onset of emulsion formation from 6.1 to 8.2 min, respectively. Increase in surfactant concentration delayed the onset of emulsification. At high cremophor EL concentration, progress of emulsification might be compromised by viscous liquid crystalline gel formed at the surfactant-water interface. It was reported that when a self-emulsified system is diluted by the aqueous phase various mesomorphic phases formed between the formula and the water. This was observed when the mesogenic properties of the formulation at different concentrations of each component were evaluated by studying the optical birefringence of the samples. In the absence of water, a droplet of surfactant (cremophor EL) and co-surfactant (capmul MCM-C8) placed in contact on a microscope slide revealed a boundary with no obvious signs of mixing and no optical birefringence. When cremophor EL was mixed with water in the absence of co-surfactant, the mixture showed birefringent texture of a gel.

Addition of co-surfactant resulted in typical birefringent textures of non-gelled fluid lyotropic liquid crystalline phase for a system with a fixed surfactant to co-surfactant weight ratio of 1:1.

5 [0054] As shown in FIG. 8(b), a cumulative percent of the formulation emulsified with time could be obtain by plotting cumulative  $NTU_{plateau}$  as a function of time, assuming that  $NTU_{plateau}$  reflect 100% of the formula released from the capsules regardless of the actual amount of CoQ<sub>10</sub> dissolved in the medium. As seen from FIG. 8(b), plots of cumulative percent of the formulation released with time are identical to the original profiles correlating turbidity with time where curved characteristics mainly lag time, pseudo linear phase and plateau are preserved. This, slope of the pseudo linear phase for the line correlating cumulative percent emulsified with time could be regarded as the emulsification rate ( $E_{rate}$ ) or emulsification efficacy. This value is very useful in comparing emulsification tendency of the self-emulsified preparation. FIG. 10 correlates emulsification rate with oil loading and surfactant to co-surfactant ratios.  $E_{rate}$  is given as percent of the formula emulsified per 10 minute. Maximum emulsification rate was obtained at a surfactant to co-surfactant ratio of 1 and oil loading of 42.6%.

#### EXAMPLE II

[0055] Powdered self-emulsified dosage forms provide an attractive alternative to filled-capsule preparations. The proper excipient selection, however, is crucial when formulating dry adsorbed solid formulations. The following example illustrates the various properties associated with a preferred powdered self-emulsified dosage form.

##### *Preparation of a solid-state self-nanoemulsified dosage form*

20 [0056] The eutectic-based self-nanoemulsified drug delivery system (SNEDDS) of CoQ<sub>10</sub> was prepared as follows: CoQ<sub>10</sub> and lemon oil at a ratio of 1:1 were accurately weighed into screw-capped glass vials and melted in a water bath at 37 °C. Cremophor EL and Capmul MCM-C8 were added to the oily mix, each at a final concentration of 26.9% w/w. The resultant emulsion was mixed with a stirring bar until a transparent solution of SNEDDS was obtained. The SNEDDS then was allowed to cool at ambient temperature for 24 hours until a viscous paste was obtained. Nanoemulsion-absorbed granular material was obtained from a mixture of SNEDDS paste, Kollidon VA 64, Glucidex IT 12, and Avicel at a ratio of 30 0.11:0.13:0.56:0.2, respectively. SNEDDS was mixed initially with Kollidon VA 64 using a mortar and pestle until a semisolid waxy paste was obtained. The mixture then was ground with Glucidex IT 12 in the mortar for 1 min to obtain the dry microemulsion-based granules. Finally, Avicel was added to the granules and blended in a V-blender (Patterson-Kelley Co.,



E. Stroudsburg, PA) for 5 minutes. Six formulations were made, each with a different grade of Avicel MCC.

*Carr's flowability index*

[0057] The flow properties of the solid-state powdered emulsion were determined by Carr's method. Compressibility, angle of repose, angle of spatula, and uniformity coefficient were measured.

[0058] The granular powder (10 g) was poured lightly into a 25-mL graduated cylinder. The powder was tapped until no further change in volume was observed. Powder bulk density,  $\rho_b$  ( $\text{g/cm}^3$ ), was calculated as the weight of the powder divided by its volume before tapping.

10 Powder tapped density,  $\rho_p$  ( $\text{g/cm}^3$ ), was calculated as the weight of the powder divided by its volume after tapping. The percentage of compressibility was computed from the following equation:

$$\% \text{ compressibility} = 100 \left( \frac{\rho_p - \rho_b}{\rho_p} \right)$$

[0059] The angle of repose was measured with a protractor for the heap of granules formed by passing 10 g of the sample through a funnel at a height of 8 cm from the horizontal surface. A steel spatula with a 5 X 7/8 in. blade was inserted to the bottom of the heap and withdrawn vertically. The angle of the heap formed on the spatula was measured as the angle of spatula.

[0060] The uniformity coefficient was obtained by sieve analysis of 10 g of the powdered material using a Retsch sieve shaker type AS200 (F. Kurt Retsch GmbH, Germany) fitted with eight US-standard sieves (Dual Mfg. Co., Chicago, IL) ranging in size from 0.075 to 1.7 mm. Uniformity coefficient is the numerical value arrived at by dividing the width of the sieve opening that will pass 60% of the sample by the width of the sieve opening that will pass 10% of the sample. The flowability index was calculated with the point scores, ranging from 0 to 100, in a scale described by Carr to evaluate the flow and the arching properties of powders.

*Compaction of the solid-state self-nanoemulsified dosage form*

[0061] Microemulsion-adsorbed compacts were prepared using concave elongated punches (Natoli Engineering Co., St. Charles, MO). Tablets were made by compressing 1245 mg of the powder, which corresponds to 30 mg in weight of CoQ<sub>10</sub>, between the faces of the punch. Punches were mounted between the platens of a Carver press model C (Carver Inc., Wabash, IN) attached to a semiautomatic compression assembly model 2826 (Carver). The

compaction pressure ranged from 15.6 to 312.3 MPa. The dimensions of the compact were measured to  $\pm 0.01$  mm using a dial thickness gauge (Lux Sci. Inst. Corp., New York, NY). Punches were 0.750 in. long and 0.375 in. wide and provided tablets with an area of the curved segment equivalent to 0.0083 in.<sup>2</sup> and a height of the curved surface above the central thickness equivalent to 0.06 in.

*Determination of true density and compact porosity*

[0062] The true density,  $\rho_t$ , of the powdered self-emulsified formulation was determined in triplicate using a helium pycnometer, model Ultra-pycnometer 1000 (Quantachrome, Boynton Beach, FL). The density of the resulting compacts,  $\rho_c$ , was calculated from the weight and volume of the compact. The porosity,  $\epsilon$ , of the compacts was calculated by the following equation:

$$\epsilon = 100 \left( 1 - \frac{\rho_c}{\rho_t} \right)$$

*Determination of tensile strength*

[0063] Tensile strength provides a measure of the inherent strength of the compacted material independent of tablet dimensions. Tensile strength of the elongated, curve-faced tablets was measured in triplicate with a three-point flexure test using the Instron material-testing instrument model 4442 (Instron Corp., Canton, MA). The load was applied at a rate of 25mm/min, and the fracture load was obtained from the load-displacement curve recorded using Instron software series IX. A typical load-displacement curve of the microemulsion-based tablets is shown in FIG. 11. Tablets were examined for the mode of failure, and only those with the fracture plane running through the center point of the surface of the tablet were used to derive tensile-strength values.

[0064] The tensile strength was calculated by the following equation:

$$\sigma_f = \frac{3FL}{2d^2} \left( \frac{d + 2a}{6A + bd} \right)$$

in which  $\sigma_f$  is the tensile strength;  $F$  is the fracture load in a three-point flexure test;  $b$  and  $d$  are the width and the thickness of the tablet, respectively;  $a$  is the height of the curved surface above the central thickness;  $A$  is the area of the curved segment; and  $L$  is the distance between the lower supports.

*Heckel analysis*

[0065] The densification of the dry powdered emulsion was analyzed by the out-of-die Heckel equation

$$-Ln \epsilon = K P + D$$

in which  $P$  is the compaction pressure,  $\epsilon$  is the porosity of the compact,  $K$  is the slope of the linear portion of the Heckel plot, and  $D$  is a function of the original compact volume.  $K$  is equal to the reciprocal of the mean yield pressure  $P_y$ , which is three times the yield strength of the material.  $D$  is a constant related to the geometry of the system and the degree of packing of the particles in the die.

#### *Measurement of surface roughness*

[0066] The roughness profiles for the upper and lower surfaces of the compacts were measured with a Mahr perthometer concept 6.3 surface texture-measuring instrument (Mahr Federal Inc., Cincinnati, OH). Tablets were mounted on the X/Y table and scanned with a contact PZK drive unit using the stylus method to move the tracing arm (model MFW-250) across the surface. A tracing length of 3.5 mm was used to obtain 51 profiles with a spacing of 112  $\mu\text{m}$ . P-profile, waviness, and roughness parameters were computed for every profile, and the mean of all 51 profiles was collected. The following parameters were measured:

- 15         $P_s$  (profile parameter): the mean distance between local peaks of the P-profile
- $W_s$  (waviness parameter): the mean distance between local peaks of the W-profile
- $R_a$  (roughness average): the arithmetic average of the roughness profile ordinates
- $R_z$  (mean roughness depth of the R-profile): the arithmetic average of roughness depths (i.e., the vertical distance between the highest peak and the deepest valley of consecutive sampling lengths).

[0067] P-profile (primary profile): the mean line generated from the traced profile. Using profile filters, P-profiles separate into long-wave (W-profile) and short-wave (R-profile) components. A representative surface topography, P, W, and R profiles, obtained by the profilometer are shown in FIG. 12.

#### *Friability and disintegration studies*

[0068] The friability of the compacts was measured using a VanKel type, dual-chamber drum, friability tester (VanKel, Cary, NC) set at a rotation speed of 25 rpm. Five grams of tablets were rotated for 4 min (100 rotations). At the end of the run the tablets were weighed accurately, and the percent friability was computed from the weight of tablets before and after the test. The disintegration time for three replicates was measured using the VanKel single-basket disintegration-testing system at 37 °C according to the *USP XXIV* specification.

*Dissolution studies*

[0069] The dissolution profiles of the self-emulsified tablets were determined using a *USP XXIV* rotating basket apparatus (model VK7000, VanKel) at 37 °C. The rotating speed was 50 rpm, and the dissolution medium was 900 mL of water. Samples (3 mL) withdrawn at  
 5 fixed time intervals were filtered using a 10- $\mu$ m VanKel filter and were assayed for CoQ<sub>10</sub> by HPLC at 275 nm. Briefly, CoQ<sub>10</sub> was analyzed using a C18 3.9 X 150 mm reverse-phase chromatography column (Nova-Park; Waters, Milford, MA). The mobile phase consisted of methanol-*n*-hexane (9:1) and was pumped at a flow rate of 1.5 mL/min<sup>-1</sup>. The dissolution experiments were conducted in triplicate.

10 *Evaluation of flow properties*

[0070] One of the limitations of self-emulsified tablet dosage forms is the poor flow of the powdered mass that holds the oily formulation. The flowability index shown in Table 3 for the microemulsion-absorbed powdered material was obtained by measuring the powders' mechanical properties (i.e., compressibility, angle of repose, angle of spatula, and uniformity  
 15 coefficient as previously discussed).

Table 3

Avicel MCC grade	Disintegration Time (min)	<u>Tensile Strength</u>		<u>Yield Strength</u>		Flowability Index
		$\sigma_0$ (MPa)	R <sup>2</sup>	(MPa)	R <sup>2</sup>	
Avicel PH-105	47.82 (0.66)	0.26098	0.987	14.3062	0.994	56.5
Avicel PH-101	30.65 (0.65)	0.35876	0.989	14.368	0.992	63.5
Avicel PH-113	27.88 (1.5)	0.32991	0.997	25.0627	0.948	59
Avicel PH-102	22.775 (1.275)	0.32834	0.991	14.43	0.991	55
Avicel PH-112	23.475 (1.975)	0.38837	0.992	30.8642	0.97	63
Avicel PH-200	15.94 (1.54)	0.34455	0.992	20.202	0.951	52

According to the method proposed by Carr, the flowability performance of a powder with a flow index between 60 and 69 can be described as acceptable. A higher value would indicate a still-better flow, but considering high oil loading in the formulation, the flow values obtained are reasonably good. For direct compression, these values can be improved readily

- 5 by adding a low concentration of silicates such as silicon dioxide, commonly used as a glidant and anti-adherent. Good flow is the result of the granular nature of the formulations, which is enhanced primarily by the absorbing properties of Kollidon VA 64. The effect of MCC particle size on the flow properties of the preparations appeared insignificant.

*Heckel analysis of the powdered self-emulsified formulation*

- 10 [0071] The Heckel equation is used often to distinguish between the mechanisms of consolidation such as plastic deformation and brittle fracture. Three types of Heckel plots were reported that distinguish between the compaction behavior of powdered material on the basis of their particle size or mixture components. Data required for Heckel analysis are obtained by either out-of-die or in-die methods. The in-die or at-pressure method collects
- 15 data during the compaction of the powder. On the other hand, the out-of-die or zero-pressure method requires collecting data after the ejection of the compacts, a procedure that eliminates the effect of elastic deformation on the densification of the powder.

- [0072] The out-of-die Heckel analysis of the compaction of the microemulsion-absorbed granules containing various grades of MCC is shown in FIG. 13. The Heckel plots appear to
- 20 be linear over the compaction range between 15.6 and 312.3 MPa. Linear regression was performed on the data points of all the powdered materials to calculate the yield strength as previously discussed. Yield strength (see Table 3) increased by increasing the particle size of MCC grades having a 5% moisture content. This may be attributed to the effects of the initial particle size on volume reduction. In addition, absorbing oil into the surface of the powder
- 25 may alter its compaction properties.

- [0073] Several other researchers reported that coating the particles of various pharmaceutical powders with layers of surfactant noticeably alters their mechanical behavior when they are compressed into tablets. The degree of coating depends on the available surface area and the absorbing capacity of the powder. Formulations made with Avicel PH-105 had the lowest
- 30 yield strength at 14.3 MPa (see Table 3). This probably is a result of the smaller particle size of Avicel PH-105, which provides a larger surface area for adsorption. This in turn facilitates homogeneous oil distribution throughout the compact, allows efficient particle lubrication and packing, and mediates plastic deformation. Formulations made with Avicel PH-112 and 113 had the highest yield-strength value among the compacts. Avicel PH-112 and 113 have a

moisture content of no more than 1.5% and 2% respectively. The reason for the higher yield-strength value is still unclear. It might be the result of moisture-mediated surface absorption, which limits the formulations' absorbing capacity. In one reported study, moisture was found to act as a plasticizer and to influence the mechanical properties of MCC. Such a

5 phenomenon might help retain surface characteristics and preserve tableting and compaction properties of adjuvants. The adjuvants, Avicel PH-112 and 113, were added merely to boost the compressibility of the soft oil-absorbed compacts rather than promote oil absorption.

*Tableting performance of the powdered self-emulsified formulations*

[0074] To describe the tableting performance of the powdered microemulsion,  
10 compressibility, compatibility, and tableability of the formulations were evaluated.

[0075] Compressibility is the ability of a powdered material to undergo a reduction in porosity as a result of applied pressure. This could be represented by a plot of porosity against the applied compaction pressure, as shown in FIG. 14. Compressibility of the powders is an important factor that governs the strength of compacts, especially at lower  
15 compaction pressures. This effect is the result of the formation of a larger interparticulate bonding area and a reduction in porosity that arises from plastic deformation. Hence, the more compressible the powder, the stronger the resultant compacts. When the dry powdered microemulsion-based formulations were compressed under the same compression conditions, compacts made with Avicel PH-105 had the lowest porosity and thus were the most  
20 compressible among the adsorbed powders. This result might be attributed to the greater plasticity of the formulation containing Avicel PH-105 as indicated by its low yield strength of 14.3 MPa (see Table 3). The outcome also may be the result of the smaller particle size (20  $\mu\text{m}$ ) of Avicel PH-105. Smaller particle size provides larger surface areas for oil adsorption and allows the powder to pack more efficiently. Avicel PH-112 and 113 showed  
25 the greatest resistance to plastic deformation at a lower compaction pressure, as observed by their higher yield strengths of 30.9 and 25.1 MPa, respectively (see Table 3). Nevertheless, all the formalities showed great dependence on compression pressure regardless of MCC particle size. The porosity of all powdered materials decreased rapidly with an increase in compaction pressure  $\leq 120$  MPa and reached relatively constant values thereafter.

30 [0076] Compactibility is the ability of a powdered material to produce compacts with sufficient strength under the effect densification. This can be represented by a plot of tablet tensile strength against the resultant porosity, at which tensile strength decreases exponentially with an increase in porosity, as shown in FIG. 15. This relationship can be expressed by the following equation:

$$Ln\sigma = Ln\sigma_0 - b\epsilon$$

in which  $\sigma$  is the tensile strength,  $\sigma_0$  is the tensile strength at zero porosity,  $b$  is a constant related to the pore distribution in the tablets, and  $\epsilon$  is the porosity. Tensile strength at zero porosity,  $\sigma_0$ , was obtained by fitting the equation to the data followed by extrapolation. All powdered formulations followed the exponential relationship described in the equation. Tensile strength at zero porosity,  $\sigma_0$ , (see Table 3) appears independent of the initial MCC particle size. The lowest  $\sigma_0$  value for compacts made with Avicel PH-105 indicates the weakest bonding, which can be attributed to its highest adsorbing capacity. This causes Avicel PH-105 particles to be fully coated with a film of the oily formulation, thereby reducing the ability for interparticulate interactions and surface bonding.

[0077] Tabletability is the ability of a powdered material to produce compacts with sufficient strength under the effect of compaction pressure and is represented by a plot of tablet tensile strength against compression pressure. A linear relationship between tensile strength and compaction pressure was observed for each of the formulations within the compaction range <120 MPa and reached a plateau thereafter, see FIG. 16. The effect of particle size of MCC on tensile strength appears less significant throughout the compaction range. MCC characteristics such as particle size and size distribution were found to have little effect on the tensile strength of tablets made from spray-dried Avicel. This could result from the low MCC loading of 20% in the formulation. The adsorbing capacity of MCC appeared insignificant in terms of producing compacts with distinctive tensile strengths at lower compaction pressures. At compression loads >120 MPa, during which most of the pores are eliminated, the difference in the interparticulate bonding area would be small. At a higher compression pressure, the bonding strength per unit bonding area would be the decisive factor in controlling compact strength. Consequently, Avicel PH-101, 112, and 200 showed the greater tensile strengths of 0.36, 0.39, and 0.34, respectively, at compaction pressures >120 MPa.

#### *Surface roughness study*

[0078] The profile parameters measured for the compacts are listed in Table 4.

30

Table 4

Avicel MCC Grade	P-Profile		W-profile		R-Profile			
	$P_s$ ( $\mu\text{m}$ )		$W_s$ ( $\mu\text{m}$ )		$R_a$ ( $\mu\text{m}$ )		$R_z$ ( $\mu\text{m}$ )	
	Upper	Lower	Upper	Lower	Upper	Lower	Upper	Lower
Avicel PH-105	118.2	151.68	391.02	446.9	2.97	1.83	20.07	12.84
Avicel PH-101	123.82	157.09	373.9	486.62	1.84	1.63	12.92	11.6
Avicel PH-113	143.6	144.24	384.26	427.14	1.96	1.84	14.26	13.08
Avicel PH-102	156.78	173.51	386.88	469.76	1.48	1.31	10.62	9.26
Avicel PH-112	152.31	160.58	357.12	405.87	1.85	1.59	13.53	10.91
Avicel PH-200	162.34	175.16	387.62	431.95	1.77	1.52	12.57	11.04

Waviness of the lower surface of the tablets, exposed to the lower punch during compaction, was greater than that of the upper surface of the compacts. This is apparent from the W and P profiles given as  $W_s$  and  $P_s$  parameters, respectively. Higher values of the  $W_s$  parameter for the lower surface of the tablets might be the result of the segregation of the larger granules to the bottom of the die during powder filling. These granules are the Kollidon VA 64-based paste ground with maltodextrin. Segregation was visually evident by the higher degree of mottling of the lower surface caused by the colored granules when compared with the extragranular white MCC powder. However, no change in surface waviness was observed as a function of the initial MCC particle size.

[0079] On the other hand, the P-profile measures both roughness and waviness of the surface. Both granule segregation and MCC particle size induced the  $P_s$  parameter, which is a measure of the distance between grooves primarily caused by granules of variable sizes. Higher  $P_s$  values of the lower surface of the compacts indicate that surface waviness is the dominant factor in determining the  $P_s$  parameter.  $P_s$  increased with an increase in particle size from Avicel PH-105 to Avicel PH-200. This is probably because larger-size MCC provides greater spacing between the particles. Because of the powder segregation, the lower punch is exposed to a larger portion of the granules that contain the lipid-based formulation. This in turn provides lubrication to the surface of the punch during tablet compaction and ejection. As a consequence, the roughness profile of the lower surface of the compacts given as  $R_a$  and  $R_z$  was lower than that of the upper surface of the tablets exposed to the less-lubricated upper punch. However, the MCC particle size was less significant in terms of the roughness parameters. This outcome is attributable to the fact that  $R_a$  and  $R_z$  are measures of the heights



and depths of the peaks and valleys formed on the surface of the tablets as a result of powder compaction. Plastic deformation might have diminished the differences between MCC particles when they were monitored vertically yet maintained their characteristic boundaries detected by the P-profile parameters.

5 *Friability study*

[0080] Friability of the compacts made from the powdered self-emulsified system as a function of compaction pressure is shown in FIG. 17. Friability decreased gradually with an increase in compression load and reached a plateau of <0.1% at compression pressures >120 MPa independent of the initial MCC particle size. No effect of MCC grade and size was  
10 evident in terms of the friability of the compacts. This correlates well with the compressibility and tabletability data. Porosities and tensile strengths for all the preparations reached their optimum values at 120 Mpa, reflecting the greatest interparticulate bonding that was further induced by oil bridging the particles

*Dissolution study*

15 [0081] To evaluate the emulsion release from the absorbing compacts, dissolution studies were performed for tablets prepared at a low compaction pressure of 31.2 MPa. Ideally, SNEDDS should be released from the tablets and completely emulsify into the dissolution medium. This effect was evaluated by measuring the cumulative percent of the drug solubilized into the aqueous medium as part of the released emulsion. Dissolution plots of  
20 the self-emulsified tablets are shown in FIG. 18. The dissolution rate within the first 45 min appeared to be dependent on MCC particle size. The cumulative percent of CoQ<sub>10</sub> solubilized in 45 min for compacts made with Avicel PH-200, 102, 112, 113, 101 and 105 was 51.5, 49, 44, 39.5, 36, and 8.7%, respectively. After 1 hour, dissolution reached a plateau with an average release of 55% (except for Avicel PH-105). Poor CoQ<sub>10</sub> dissolution  
25 might be the result of an irreversible hydrophobic interaction between CoQ<sub>10</sub> and MCC. Initial powder compaction and slow disintegration (see Table 3) also might have induced irreversible surface adsorption to the soluble excipients of the formulation. This process causes variable release rates. Oily components of the formulation are emulsified into the aqueous medium at a faster rate compared with the release of CoQ<sub>10</sub>. However, tablets made  
30 with Avicel PH-105 induced sustained release of CoQ<sub>10</sub> in a time span of 6 hours. As previously discussed, tablets made with Avicel PH-105 had the least yield and tensile strength and the lengthiest disintegration time (see Table 3). This suggests oil-induced bridging and sticking between the Avicel particles, an outcome that provides a greater area of

contact. The increase in the cohesion between the particles accounts for delayed release rates without increasing the hardness of the tablets.

[0082] Although the present invention has been disclosed in terms of a preferred embodiment, it will be understood that numerous additional modifications and variations  
5 could be made thereto without departing from the scope of the invention as defined by the following claims.

What is claimed is:

1. A self-nanoemulsified drug delivery system, comprising
  - a) 19-26 wt.% of a pharmacologically effective drug;
  - b) 23-31 wt% polyoxyl 35 castor oil;
  - 5 c) 23-31 wt. % of a medium chain mono- and diglyceride; and
  - d) 19-26 wt. % of an essential oil.
2. The self-nanoemulsified drug delivery system of claim 1, wherein said pharmacologically effective drug is selected from the group comprising ubiquinone,  
10 cyclosporine, and Vitamin E.
3. The self-nanoemulsified drug delivery system of claim 2, wherein said pharmacologically effective drug is ubiquinone.
- 15 4. The self-nanoemulsified drug delivery system of claim 3, wherein said essential oil is lemon oil.
5. The self-nanoemulsified drug delivery system of claim 4, comprising
  - a) about 23 wt.% ubiquinone;
  - 20 b) about 27 wt.% polyoxyl 35 castor oil;
  - c) about 27 wt.% a medium chain mono- and diglyceride; and
  - d) about 23 wt.% lemon oil.
6. A capsule formulation, comprising the self-nanoemulsified drug delivery system of  
25 claim 5.
7. The self-nanoemulsified drug delivery system of claim 1, wherein said essential oil is selected from the group comprising menthol, spearmint oil, peppermint oil, lemon oil, anise oils, and mixtures thereof.
- 30 8. The self-nanoemulsified drug delivery system of claim 7, wherein said essential oil is lemon oil.

9. The self-nanoemulsified drug delivery system of claim 1, wherein said polyoxyl 35 castor oil and said medium chain mono- and diglyceride are present in a ratio of 0.5 to 1.5.

10. A capsule formulation, comprising the self-nanoemulsified drug delivery system  
5 of claim 1.

11. A solid dosage form, comprising  
a) 3-35 wt.% of a copolymer of vinylpyrrolidone and vinyl acetate;  
b) 11-47 wt.% microcrystalline cellulose;  
10 c) 35-82 wt.% maltodextrin; and  
d) an effective amount of said self-nanoemulsified drug delivery system of claim 1 for administering said pharmacologically effective drug to a patient.

12. The solid dosage form of claim 11, wherein said pharmacologically effective  
15 drug is selected from the group comprising ubiquinone, cyclosporine, and Vitamin E.

13. The solid dosage form of claim 12, wherein said pharmacologically effective drug is ubiquinone.

20 14. The solid dosage form of claim 11, wherein said essential oil is selected from the group comprising menthol, spearmint oil, peppermint oil, lemon oil, anise oils, and mixtures thereof.

25 15. The solid dosage form of claim 14, wherein said essential oil is lemon oil.

16. The solid dosage form of claim 11, comprising  
a) 7.8 wt.% of said copolymer of vinylpyrrolidone and vinyl acetate,  
b) 11.7 wt.% microcrystalline cellulose,  
c) 65.4 wt.% maltodextrin, and  
30 d) 15.1 wt.% of said self-nanoemulsified drug delivery system.

17. The solid dosage form of claim 11, wherein 46.1-91.1 wt.% of said pharmacologically effective drug is emulsified in a dissolution medium within 45 minutes.

18. The solid dosage form of claim 17, wherein said pharmacologically effective drug is ubiquinone.

19. The solid dosage form of claim 11, wherein said pharmacologically effective  
5 drug is ubiquinone and said essential oil is lemon oil.

20. The solid dosage form of claim 19, wherein said self-nanoemulsified drug delivery system comprises,

- a) about 23 wt.% ubiquinone;
- 10 b) about 27 wt.% polyoxyl 35 castor oil;
- c) about 27 wt.% medium chain mono- and diglyderide; and
- d) about 23 wt.% lemon oil.

15

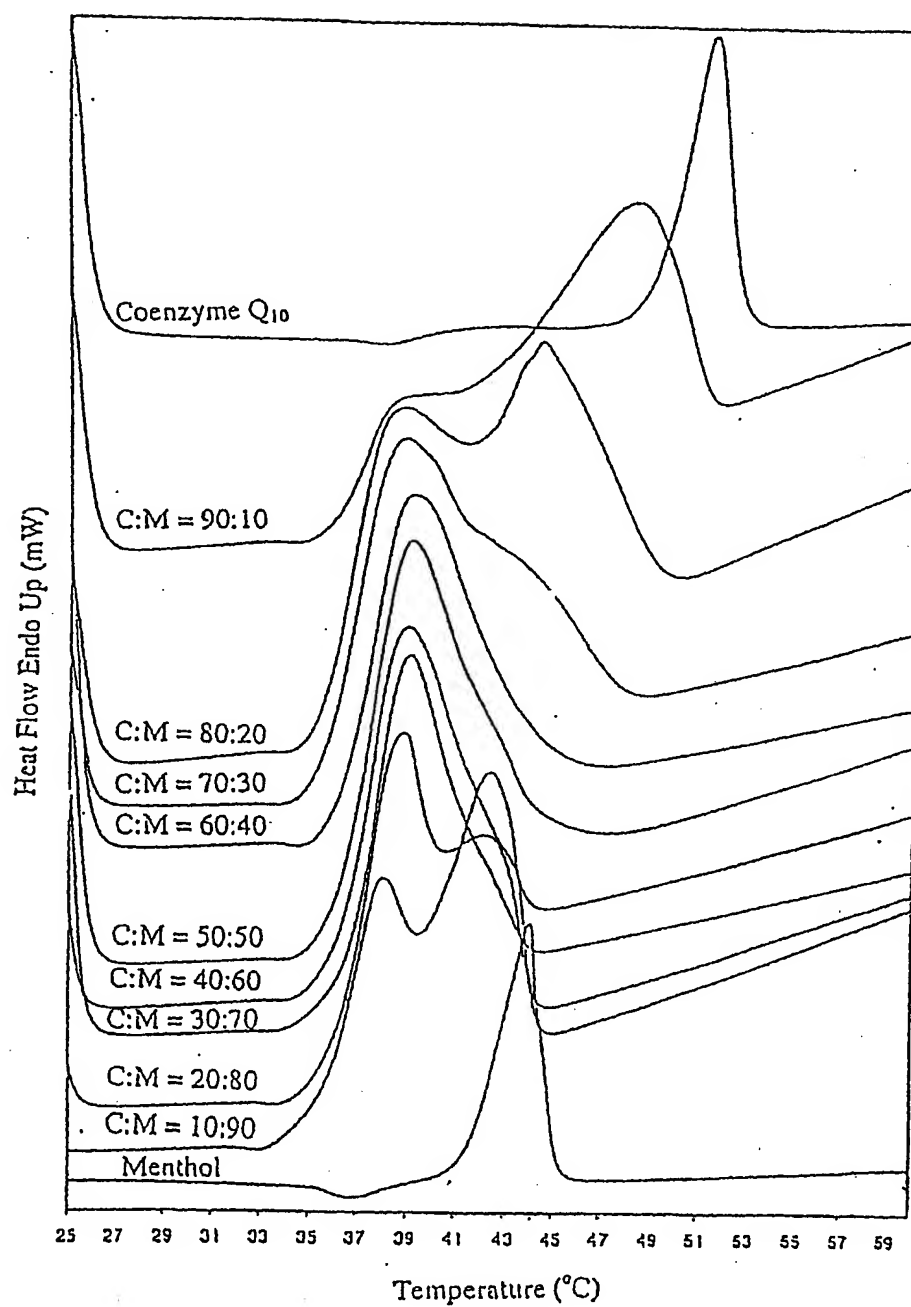


FIG. 1

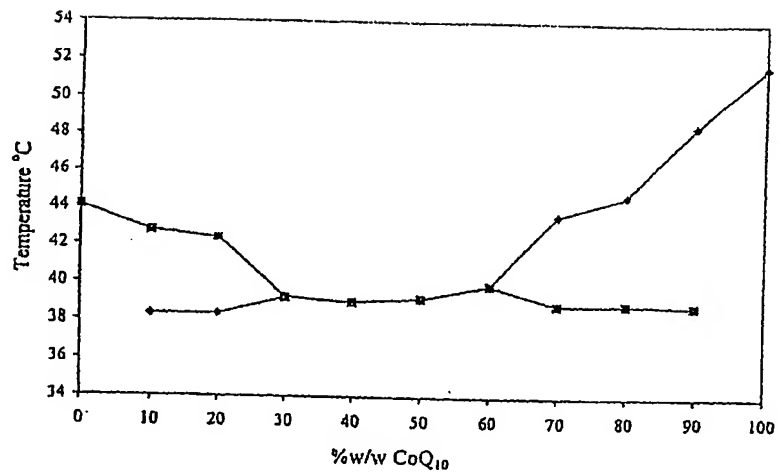


FIG. 2

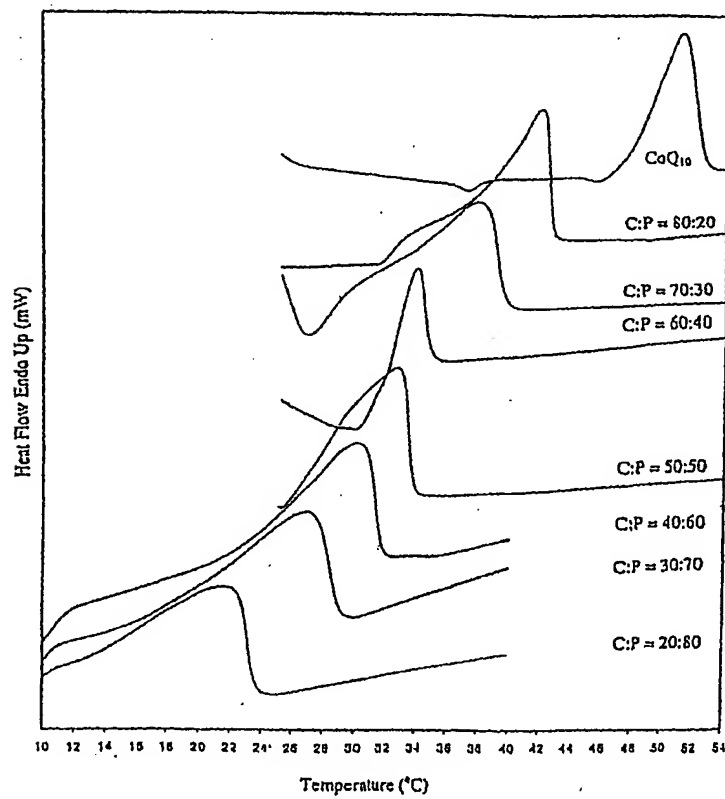


FIG. 3

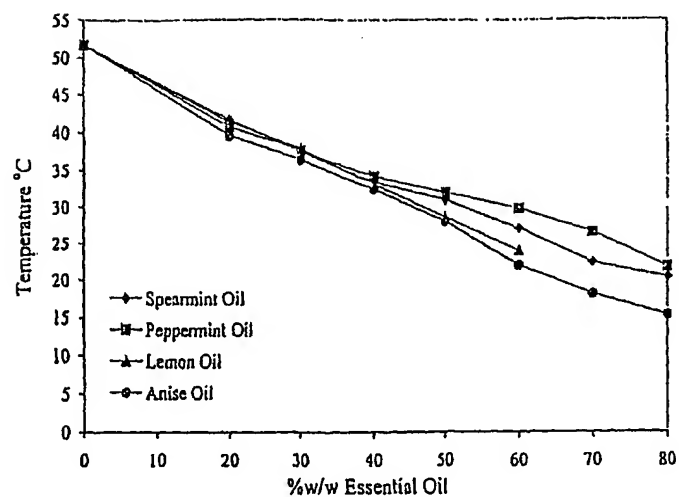


FIG. 4

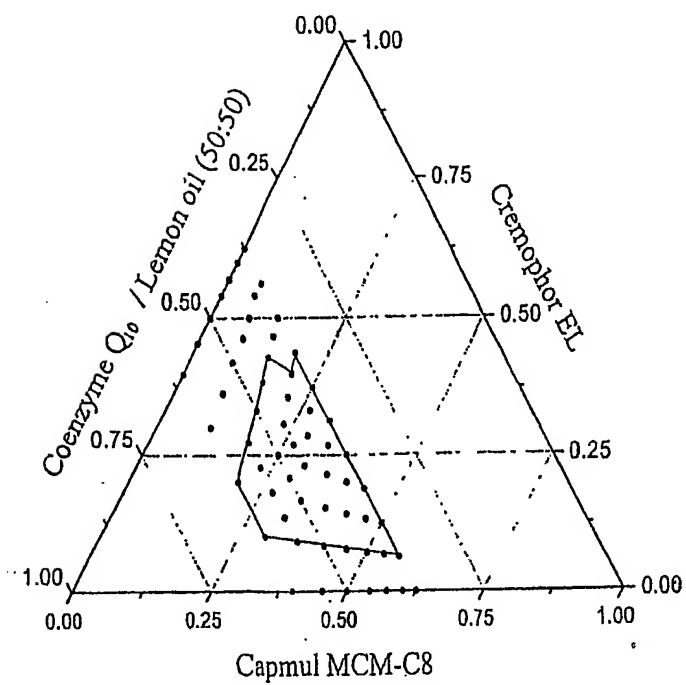


FIG. 5



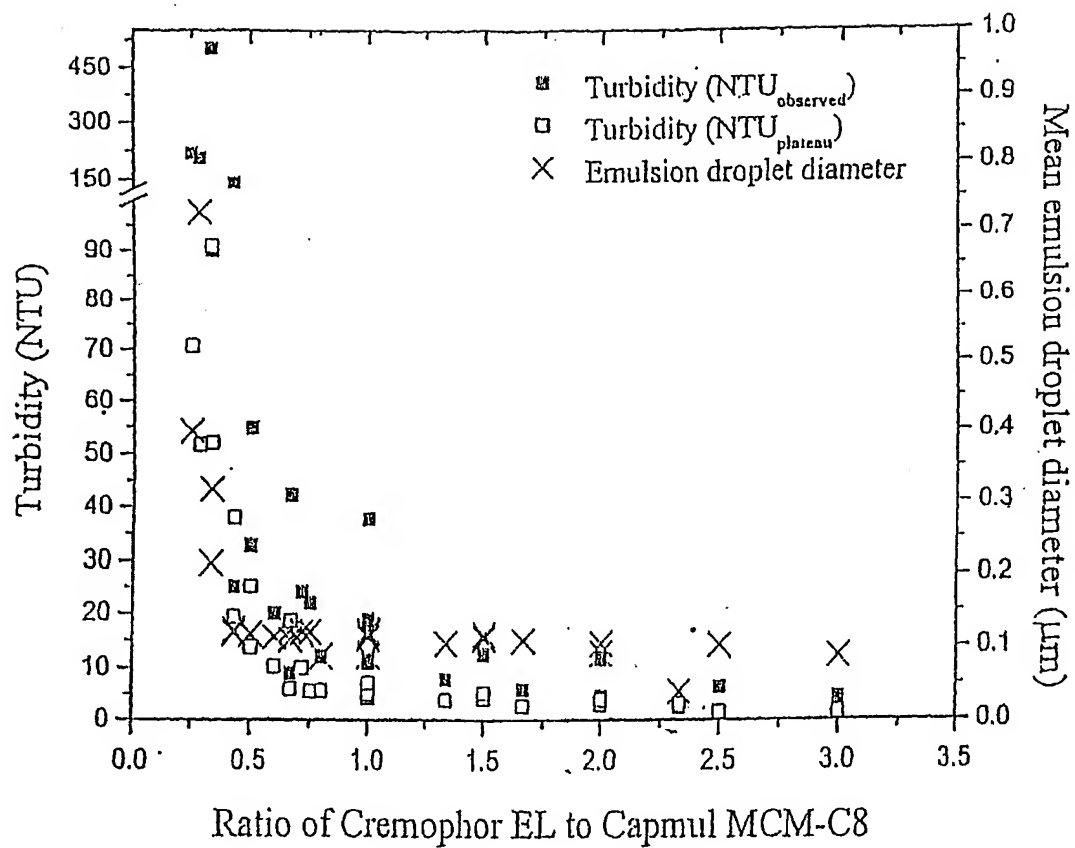


FIG. 6

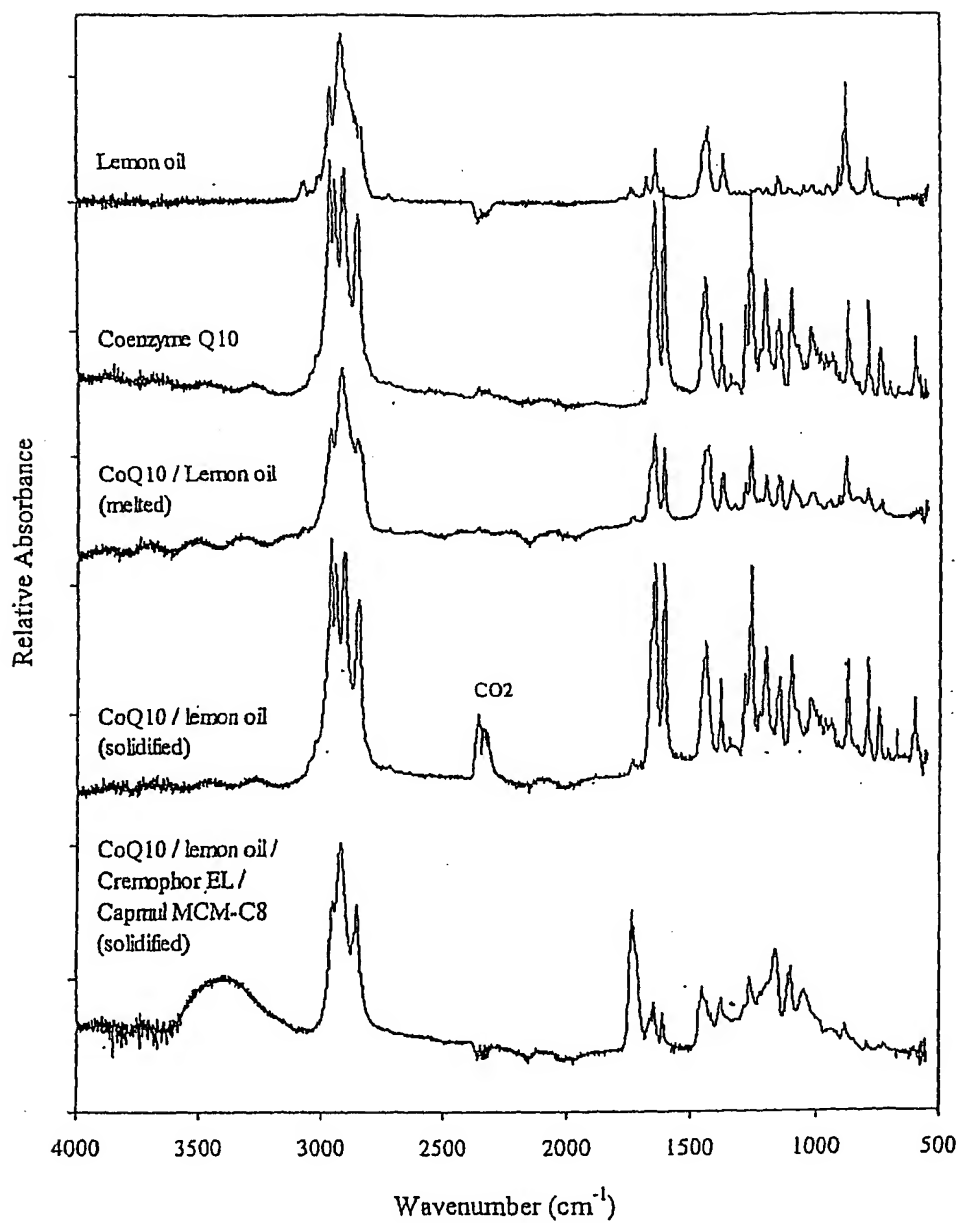


FIG. 7

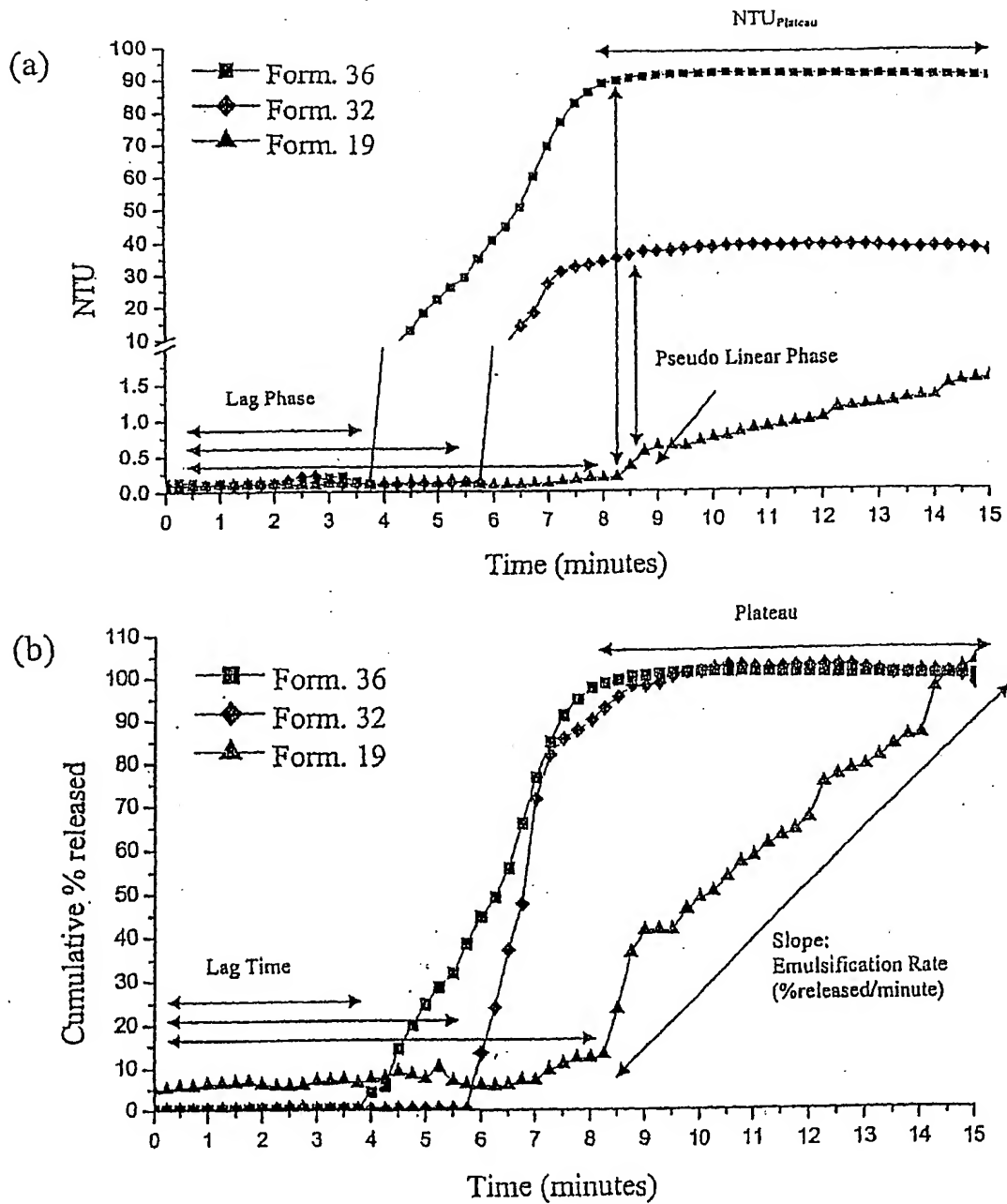


FIG. 8

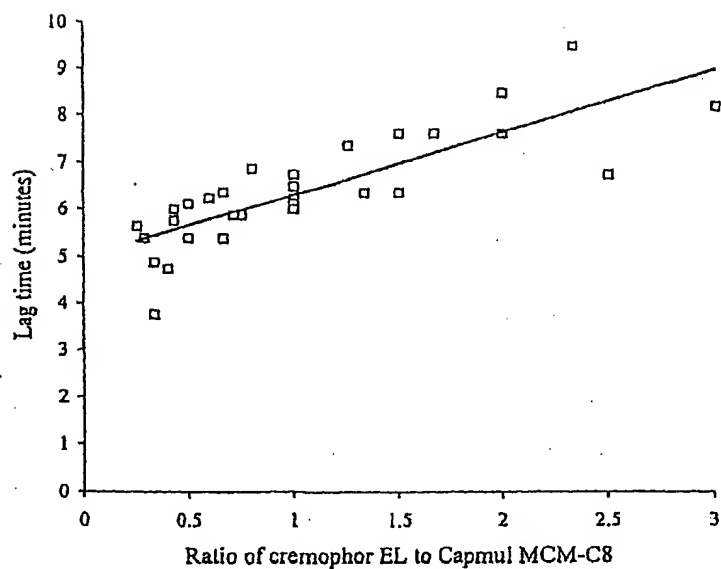


FIG. 9

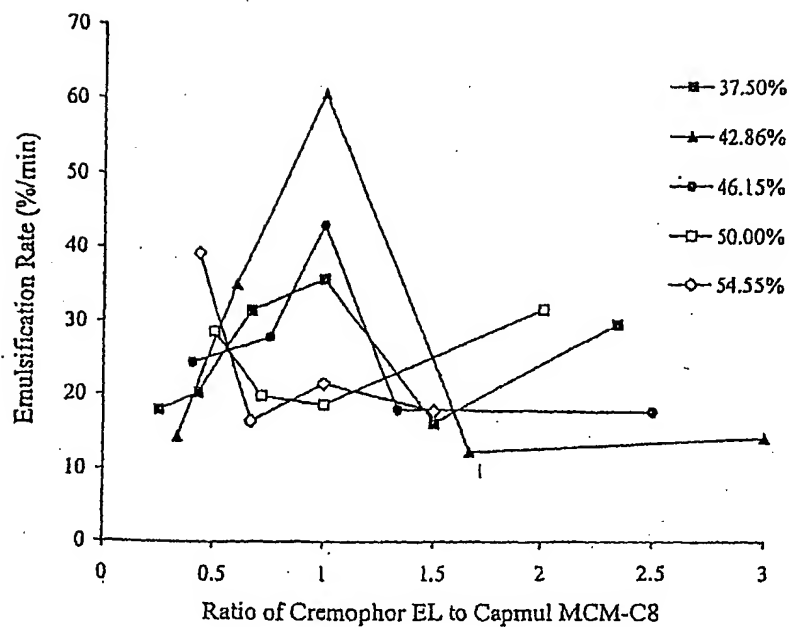


FIG. 10

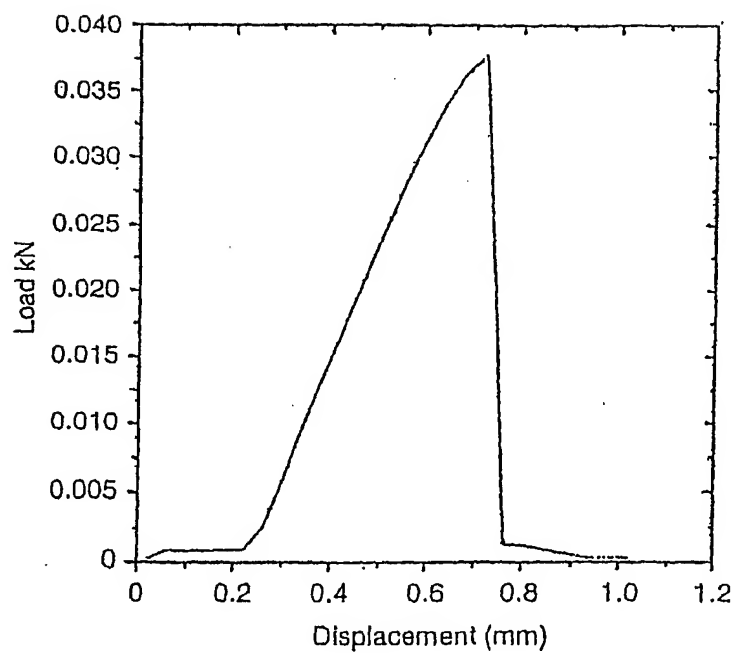


FIG. 11

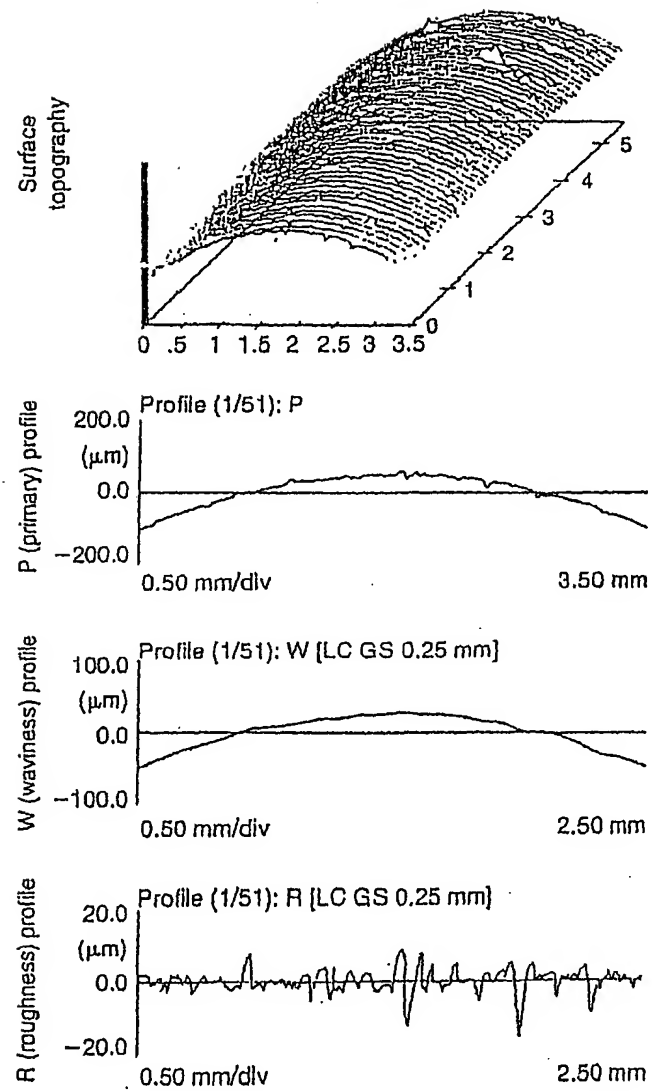


FIG. 12

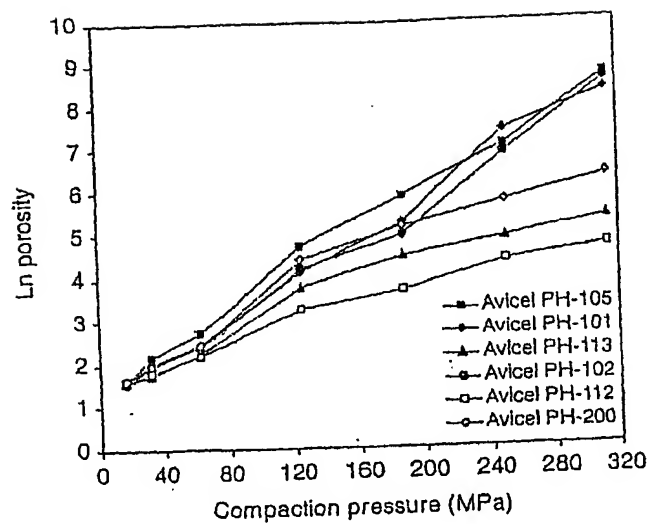


FIG. 13

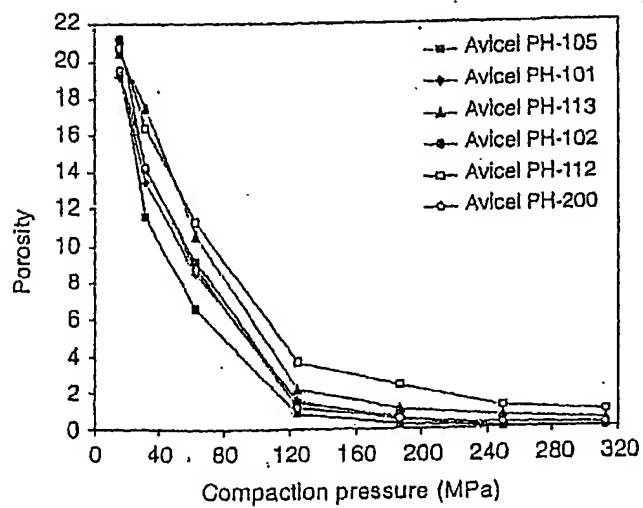


FIG. 14

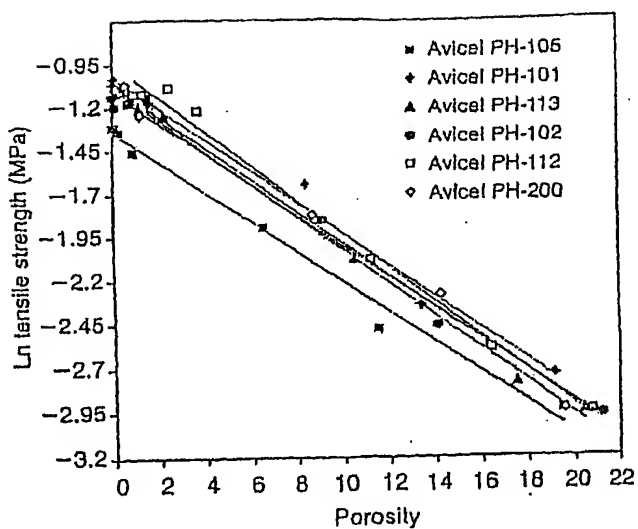


FIG. 15

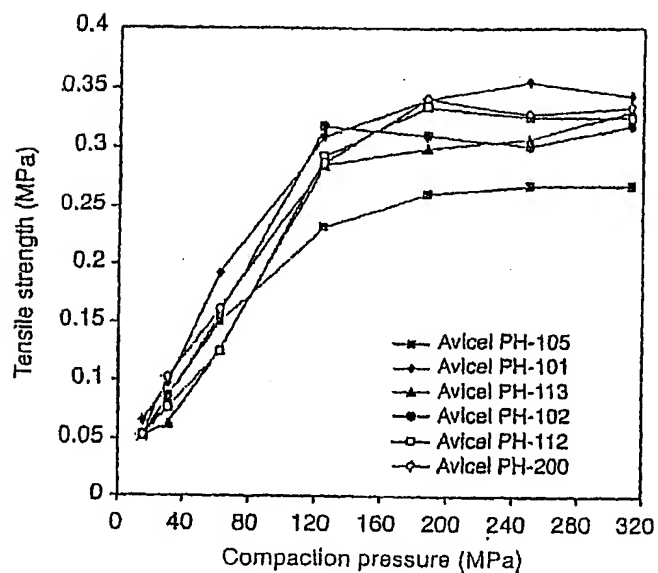


FIG. 16



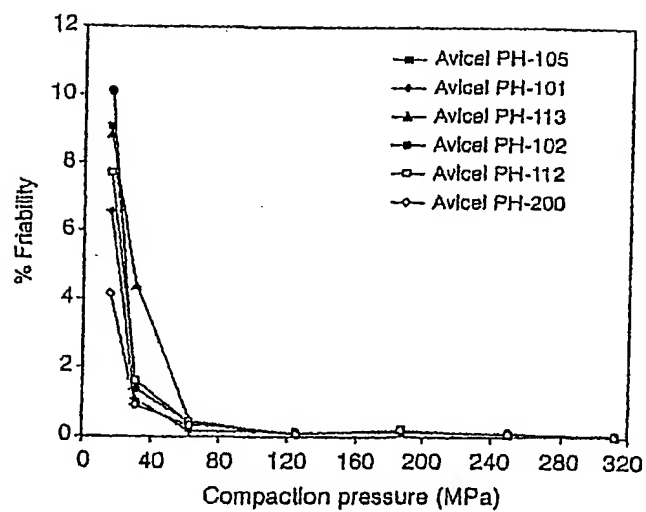


FIG. 17

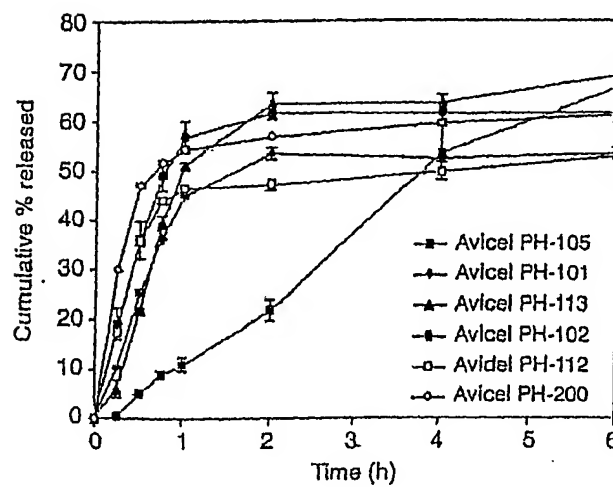


FIG. 18

**THIS PAGE BLANK (USPTO)**